www.ijiarec.com

ISSN:2348-2079

Volume-7 Issue-1

International Journal of Intellectual Advancements and Research in Engineering Computations

Segmentation of lung field from saliency maps by convolution neural network in chest radiographs using machine learning

M.Manimegalai[1], R.Suruthi[2], M.Usha[2], G.Vijayalakshmi[2], K.Vijayalakshmi[2]

[1]Assistant Professor, Department of ECE, Mahendra Engineering College for Women.

[2]UG Scholars, Department of ECE, Mahendra Engineering College for Women.

ABSTRACT

Segmenting lung fields from CXRs (Chest Radiographs) is an important task for the analysis, diagnosis and treatment of tumor diseases. Although many segmentation method have been presented. This paper proposed for the CXRs and also for lung field in Saliency Map by using Convolution Neural Network and Thresholding for lungs. In our convolutional neural network to achieve feature extraction and classification using Machine Learning Algorithm also reduce time consumption, deliver better segmentation. In this study, we implemented a Fully Convolutional Network to simultaneously segment multiple structures, namely lung field in standard Posterior-Anterior chest radiographs. We have developed a multi scale CNN approach for segmenting lung tumors which enables accurate measurement of tumor volumes in the lung. And we are executing our method via ordinary laptop. In this method reducing time consumption, give clear shape of tumor level in lung and efficiency. Achieve very higher accuracy on most of the structure when compared with state of other segmentation method.

INTRODUCTION

Volumetric lung tumor segmentation and accurate longitudinal tracking of tumor volume changes from computed tomography (CT) images are essential for monitoring tumor response to therapy. Hence, we developed two multiple resolution residually connected network (MRRN) formulations called incremental- MRRN and dense-MRRN. Our networks simultaneously combine features across multiple image resolution and feature levels through residual connections to detect and segment lung tumors. We evaluated our method on a total of1210 non-small cell (NSCLC) lung tumors and nodules from three datasets consisting of 377 tumors from the open-source Cancer Imaging Archive (TCIA), 304 advanced stage NSCLC treated with anti- PD-1 checkpoint immunotherapy from internal institution MSKCC dataset, and 529 lung nodules from the Lung Image Database Consortium (LIDC). The algorithm was trained using the 377 tumors from the TCIA dataset and validated on the MSKCC and tested on LIDC datasets. The segmentation accuracy compared to expert delineations was evaluated by computing the Dice Similarity Coefficient (DSC), distances, sensitivity and precision metrics. Our best performing incremental-MRRN method produced the highest DSC of0.74±0.13 for TCIA, 0.75±0.12 for MSKCC and 0.68±0.23 for the LIDC datasets. There was no significant difference in the estimations of volumetric tumor changes computed using the incremental-MRRN method compared with expert segmentation. In summary, we have developed a multi-scale CNN approach for volumetrically segmenting lung tumors which enables accurate, automated identification of serial measurement of tumor volumes in the lung.

Author for correspondence:
Department of ECE, Mahendra Engineering College for Women.

METHODOLOGY

The tumors in the TCIA and MSKCC were confirmed advanced stage malignant tumors while those from the LIDC were lung nodules (>3mm and confirmed by at least 1radiologist) with varying degrees of malignancy. The MSKCC dataset also included longitudinal CT scans imaged before and every 9 week during therapy up to a maximum of 17 weeks after treatment initiation. The training (TCIA) and validation set (MSKCC) consisted of contrast enhanced CT scans while the testing set from the LIDC included both regular dose and low-dose CT images. Tumor contours for the TCIA were verified and edited when necessary by radiologist (L.C.J). All ground truth tumor contours in the MSKCC dataset were confirmed by a chest radiologist (DH) with several years of experience reviewing chest CT images. The LIDC datasets were manually delineated by four radiologists who also assigned a malignancy score between 1-5 with 1 being low and 5 being high malignancy. Out of 2669, 928 were confirmed and delineated by all four radiologists and were at least 3mm in diameter. As used in prior works.

We only analyzed 529 nodules of the 928 that were assigned an average malignancy score of >3. This resulted in a total of1210 analyzed tumors from all the three datasets. There was a wide variation in the size and distribution of tumors between the datasets. The tumors in the TCIA dataset ranged in size from 1.88cc to 1033cc, MSKCC from 2.96cc to413.8cc, and the LIDC from 0.031cc to 19.18cc (all calculated according to radiologist delineation). The distribution of tumor sizes discretized by size is shown in Table I. Finally, predominant lesions in the TCIA and MSKCC dataset were located in the mediastinum or attached to chest wall while the tumors in LIDC were the most frequent in the lung parenchyma [1-5].

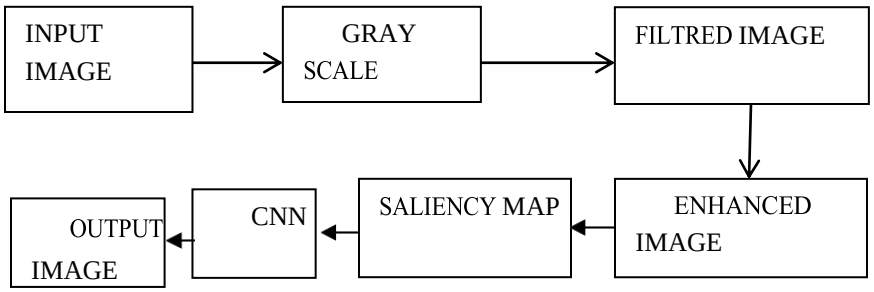

FIG.2.1 PROPOSED SYSTEM

IMAGE SEGMENTATION

INUPUT IMAGE

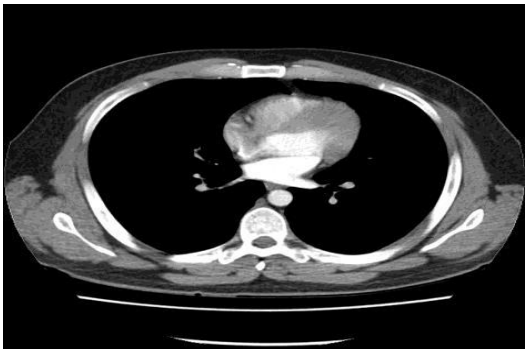

INTENSITYIMAGE(grayscale image)

This is the equivalent to a "gray scale image" and this is the image we will mostly work with in this course. It represents an image as a matrix where every element has a value corresponding to

how bright/dark the pixel at the corresponding position should be colored. There are two ways to represent the number that represents the brightness of the pixel: The double class (or data type). This assigns a floating number ("a number with decimals") between 0 and 1 to each pixel. The value 0 corresponds to black and the value 1 corresponds to white. The other class is called uint8 which assigns an integer between 0 and 255 to represent the brightness of a pixel. The value 0 corresponds to black and 255 to white. The class uint8 only requires roughly 1/8 of the storage compared to the class double. On the other hand, many mathematical functions can only be applied to the double class. We will see later how to convert between double and uint8.

FILTERED IMAGE

A Filtering is a technique for modifying image .we using median filter to converting digital image .It is a preprocessing [6-8].

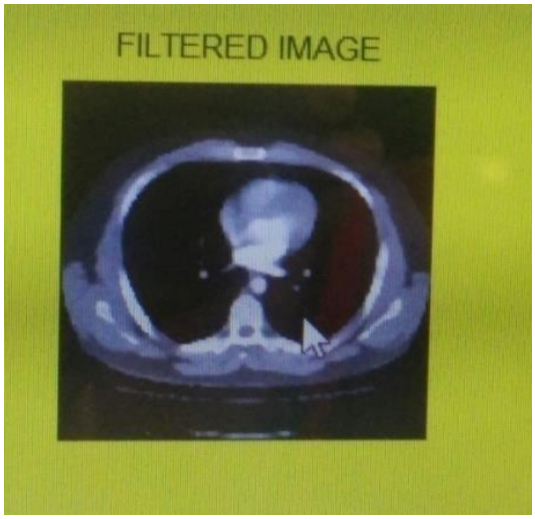

ENHANCED IMAGE

Image enhancement is to improve the interpretability or preconception of information in images for human viewers to provide better image.

SEGMENTED IMAGE

Image segmentation is a process of partitioning a digital image into multiple segments (set of pixel also known as super pixel).

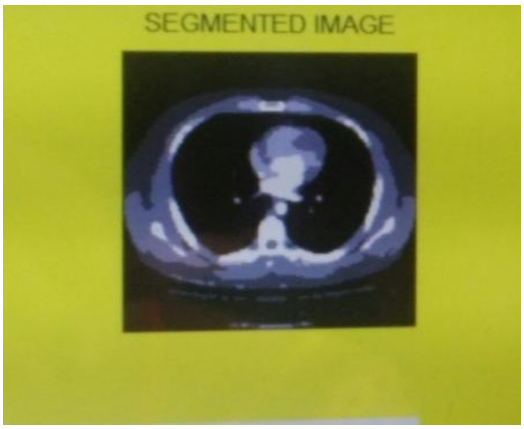

CLASSIFICATIONS OF SALIENCY MAP

Saliency maps an image that shows each pixel unique quality .it has a high quality gray scale image .it is a kind of image segmentation.

LUNG DETECTION

A X-ray image of your lungs may reveal an abnormal mass (or) nodule. A CT scan can reveal small lesions in your lungs that might not be detected on X-ray sputum cytology.

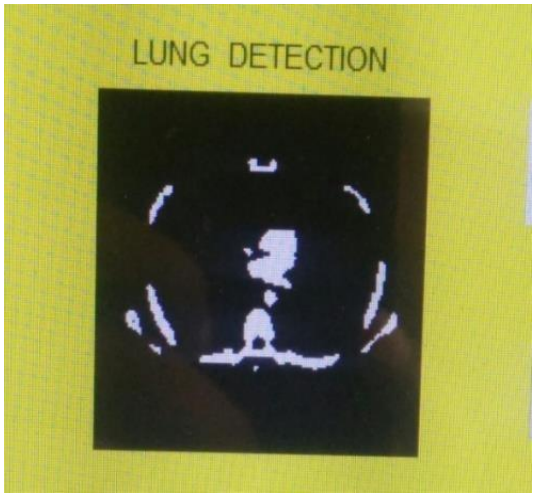

OUTPUT IMAGE

CONVOLUTIONAL NETWORK

Convolutional networks are powerful visual models that yield hierarchies of features. We show that convolutional networks by themselves, trained end-to-end, pixels-to-pixels, exceed the state-of-the-art in semantic segmentation. Our key insight is to build "fully convolutional" networks that take input of arbitrary size and produce correspondingly-sized output with efficient inference and learning. We define and detail the space of fully convolutional networks, explain their application to spatially dense prediction tasks, and draw connections to prior models. We adapt contemporary classification networks (Alex Net, the VGG net, and Google Net) into fully convolutional networks and transfer their learned representations by fine-tuning to the segmentation task. We then define a skip architecture that combines semantic information from a deep, coarse layer with appearance information from a shallow, fine layer to produce accurate and detailed segmentations. Our fully convolutional network achieves state-of-the-art segmentation of PASCAL VOC (20% relative improvement to 62.2% mean IU on 2012), NYUDv2, and SIFT Flow, while inference takes less than one fifth of a second for a typical image.

Figure1. Fully convolutional networks can efficiently learn to make dense predictions for per-pixel tasks like semantic segmentation.

FULLY CONVOLUTIONAL NETWORK

Each layer of data in a convert is a three-dimensional array of size h w d, where h and ware spatial dimensions, and d is the feature or channel dimension. The first layer is the image, with pixel size h w, and d color channels. Locations in higher layers correspond to the locations in the image they are path-connected to, which are called their receptive fields converts are built on translation invariance. Their basic components (convolution, pooling, and activation functions) operate on local input regions, and depend only on relative spatial coordinates. Writing xij for the data vector at location (i; j) in a particular layer, and yij for the following layer, these functions compute outputs yij by

Yij=fks (fxsi+ i; sj+ jg0i; j k)

Where k is called the kernel size, s is the stride or subsampling factor, and fks determines the layer type: a matrix multiplication for convolution or average pooling, a spatial max for max pooling, or an element wise nonlinearity for an activation function, and so on for other types of layers.

This functional form is maintained under composition, with kernel size and stride obeying the transformation rule.

fksgk0 s0= (f g) k0 + (k 1) s0; ss0

While a general deep net computes a general nonlinear function, a net with only layers of this form computes a nonlinear filter, which we call a deep filter or fully convolutional network. An FCN naturally operates on an input of any size, and

produces an output of corresponding (possibly resampled) spatial dimensions.

A real-valued loss function composed with an FCN de-fines a task. If the loss function is a sum over the spatial dimensions of the final layer, ‘(x ;) = Pij ‘0(xij ;), its gradient will be a sum over the gradients of each of its spatial components. Thus stochastic gradient descent on ‘computed on whole images will be the same as stochastic gradient descent on ‘0, taking all of the final layer receptive fields as a minibatch.

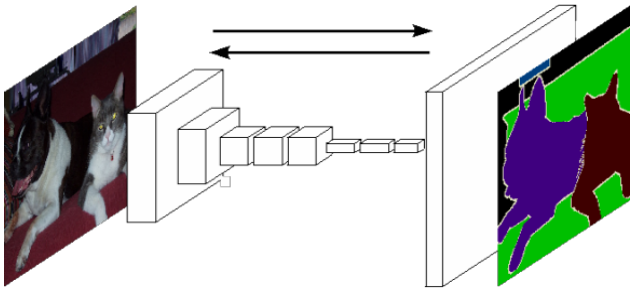

When these receptive fields overlap significantly, both feed forward computation and back propagation are much more efficient when computed layer-by-layer over an entire image instead of independently patch-by-patch. We next explain how to convert classification nets into fully convolutional nets that produce coarse output maps. For pixel wise prediction, we need to connect these coarse outputs back to the pixels. Section 3.2 describes a trick, fast scanning, introduced for this purpose. We gain insight into this trick by reinterpreting it as an equivalent network modification. As an efficient, effective alternative, we introduce deconvolution layers for up sampling in Section

In Section 3.4 we consider training by patch wise sampling, and give evidence in Section that our whole image training is faster and equally effective.

Each layer of data in a convert is a three-dimensional array of size h w d, where h and ware spatial dimensions, and d is the feature or channel dimension. The first layer is the image, with pixel size h w, and d color channels. Locations in higher layers correspond to the locations in the image they are path-connected to, which are called their receptive fields. Converts are built on translation invariance. Their basic components (convolution, pooling, and activation functions) operate on local input regions, and depend only on relative spatial coordinates. Writing xij for the data vector at location (i; j) in a particular layer, and yij for the following layer, these functions compute outputs yij by

Yij=fks (fxsi+ i; sj+ jg i; j k)

Where k is called the kernel size, s is the stride or subsampling factor, and fks determines the layer type: a matrix multiplication for convolution or average pooling, a spatial max for max pooling, or an element wise nonlinearity for an activation function, and so on for other types of layers.

This functional form is maintained under composition, with kernel size and stride obeying the transformation rule

fksgk0 s0= (f g) k0 + (k 1)s0 ;ss0

While a general deep net computes a general nonlinear function, a net with only layers of this form computes a nonlinear filter, which we call a deep filter or fully convolutional network. An FCN naturally operates on an input of any size, and produces an output of corresponding (possibly re sampled) spatial dimensions.

A real-valued loss function composed with an FCN de-fines a task. If the loss function is a sum over the spatial dimensions of the final layer, ‘(x ;) = Pij ‘0(xij;), its gradient will be a sum over the gradients of each of its spatial components. Thus stochastic gradient descent on ‘computed on whole images will be the same as stochastic gradient descent on ‘0, taking all of the final layer receptive fields as a minibatch.

When these receptive fields overlap significantly, both feed forward computation and back propagation are much more efficient when

computed layer-by-layer over an entire image instead of independently patch-by-patch.

We next explain how to convert classification nets into fully convolutional nets that produce coarse output maps. For pixel wise prediction, we need to connect these coarse outputs back to the pixels. Section 3.2 describes a trick, fast scanning, introduced for this purpose. We gain insight into this trick by reinterpreting it as an equivalent network modification. As an efficient, effective alternative, we introduce De-convolution layers for up sampling in Section.

In Section 3.4 we consider training by patch wise sampling, and give evidence in Section 4.3 that our whole image training is faster and equally effective.

KEY FEATURES

- Image enhancement, filtering, and de blurring. Image analysis, including segmentation, morphology, feature extraction, and measurement
- Spatial transformations and image registration
- Image transforms, including FFT, DCT, Radon, and fan-beam projection.
- Workflows for processing, displaying, and navigating arbitrarily large images
- Modular interactive tools, including ROI selections, histograms, and distance measurements.
- ICC color management
- Multidimensional image processing
- Image-sequence and video display
- DICOM import and export

PREPROCESSING AND POSTPROCESSING IMAGES

Image Processing Toolbox provides reference-standard algorithms for preprocessing and post processing tasks that solve frequent system problems, such as interfering noise, low dynamic range, out-of-focus optics, and the difference in color representation between input and output devices.

Image enhancement techniques in Image Processing Toolbox enable you to increase the signal-to-noise ratio and accentuate image features by modifying the colors or intensities of an image.

CONCLUSION AND FUTURE ENHANCEMENT

We proposed two neural networks to segment lung tumors from CT images by adding multiple residual streams of varying resolutions. Our results clearly demonstrate the improvement in segmentation accuracy across multiple datasets. Our approach is applicable to longitudinal tracking of tumor volumes for cancers subjected to treatment with immunotherapy, which alters both the size and appearance of tumors on CT. Given the success for lung tumors, the method is promising for other sites as well. Both of our proposed MRRN outperform existing methods.

In future the further the computation time can be reduced using different machine learning algorithm.

REFERENCES

[1]. Jemal, R. Siegel, E. Ward, Y. Hao, J. Xu, T. Murray, et al., "Cancer statistics, 2008," CA: a cancer journal for clinicians, vol. 58, pp. 71-96, 2008.

[2]. E. Eisenhauer, P. Therasse, J. Bogaerts,L. Schwartz, D. Sargent, R. Ford, et al., "New response evaluation criteria in solid tumours: revised RECIST guideline (version 1.1)," European journal of cancer, vol. 45, 2009, 228-247.

[3]. E.R.Velazquez,C.Parmar, M. Jermoumi, R. H. Mak, A. Van Baardwijk,F. M. Fennessy, et al., "Volumetric CT- based segmentation of NSCLC using 3D- Slicer," Scientific reports, 3, 2013, 3529.

[4]. Parmar, E. R. Velazquez, R. Leijenaar, M. Jermoumi, S. Carvalho, R.H. Mak, et al., "Robust radiomics feature quantification using semiautomatic volumetric segmentation," PloS one, 9, 2014, 102107.

[5]. Y. Gu, V. Kumar, L. O. Hall, D. B. Goldgof, C.-Y. Li, R. Korn, et al., "Automated delineation of lung tumors from CT images using a single click ensemble segmentation approach," Pattern Recognition, 46, 2013, 692- 702.

[6]. Y. Tan, L. H. Schwartz, and B. Zhao, "Segmentation of lung lesions on CT scans using watershed, active contours, and Markov random field," Medical physics , vol. 40, 2013, 04350.

[7]. J. Kalpathy-Cramer, B. Zhao, D. Goldgof,Y. Gu, X. Wang, H. Yang, etal., "A comparison of lung nodule segmentation algorithms: methodsand results from a multi-institutional study," Journal of digital imaging, 29, 2016, 476-487.

[8]. Y. Balagurunathan, A. Beers, J. Kalpathy-Cramer, M. McNitt-Gray, L. Hadjiiski, B. Zhao, et al., "Semi - automated pulmonary nodule interval segmentation using the NLST data Medical physics, 45, 2018, 1093-1107.

[9]. O. Grove, A. E. Berglund, M. B. Schabath, H. J. Aerts, A. Dekker, H. Wang, et al., "Quantitative computed tomographic descriptors associate tumor shape complexity and intratumor heterogeneity with prognosis in lung adenocarcinoma," PloS one, 10, 2015, 0118261.